

Atomic-scale surface demixing in a eutectic liquid BiSn alloy

Oleg G. Shpyrko,^{1,*} Alexei Yu. Grigoriev,¹ Reinhard Streitel,¹ Diego Pontoni,¹
Peter S. Pershan,¹ Moshe Deutsch,² Ben Ocko,³ Mati Meron,⁴ and Binhua Lin⁴

¹*Department of Physics and DEAS, Harvard University, Cambridge MA 02138*

²*Department of Physics, Bar-Ilan University, Ramat-Gan 52900, Israel*

³*Department of Physics, Brookhaven National Laboratory, Upton NY 11973*

⁴*CARS, University of Chicago, Chicago, IL 60637*

(Dated: September 10, 2018)

Resonant x-ray reflectivity of the surface of the liquid phase of the $\text{Bi}_{43}\text{Sn}_{57}$ eutectic alloy reveals atomic-scale demixing extending over three near-surface atomic layers. Due to the absence of underlying atomic lattice which typically defines adsorption in crystalline alloys, studies of adsorption in liquid alloys provide unique insight on interatomic interactions at the surface. The observed composition modulation could be accounted for quantitatively by the Defay-Prigogine and Strohl-King multilayer extensions of the single-layer Gibbs model, revealing a near-surface domination of the attractive Bi-Sn interaction over the entropy.

PACS numbers: 61.20.-p, 61.10.-i, 68.03.-g

The widely-accepted Gibbs adsorption rule [1] predicts the surface segregation of the lower surface energy component of a binary mixture. Liquid metals are ideal systems for studying Gibbs adsorption due to the nearly spherical shape of interacting particles, relative simplicity of the short-range interactions and the availability of bulk thermodynamic data for many binary alloys. While certain aspects of Gibbs theory can be tested through macroscopic measurements of surface tension or adsorption isotherms, very few direct measurements of the atomic-scale composition profiles of the liquid-vapor interface were reported [2, 3, 4]. In addition to fundamental questions related to surface thermodynamics of binary liquids, BiSn-based alloys have been widely studied as substitutes for Pb-based low-melting solders [5]. Thus, understanding their wetting, spreading, alloying, reactivity and other surface-related properties is of great practical importance. Moreover, interfacial phenomena dominate the properties of the increasingly important class of nanoscale materials, as demonstrated recently in studies of the liquid-solid phase stability of nanometer-sized BiSn particles [6].

Synchrotron-based x-ray reflectivity (XR) can measure the surface-normal density profile of a liquid with Ångström-scale resolution. Over the last decade XR revealed the long-predicted surface-induced atomic layering at the liquid-vapor interface for a number of elemental liquid metals [7, 8, 9, 10, 11]. *Resonant* XR near an absorption edge resolved the density profile of each component in GaIn [2], HgAu [3] and BiIn [4] liquid binary alloys. The enhancement of the concentration of the low-surface-tension component was invariably found to be confined to the topmost surface monolayer, with subsequent layers having the composition of the bulk, in accord with the simplest, and widely used, interpretation of the Gibbs rule. By contrast, we find here an atomic-scale phase separation extending over at least three atomic

layers. This is unexpected, considering the near-perfect-solution nature of the $\text{Bi}_{43}\text{Sn}_{57}$ alloy in the bulk [12, 13].

A liquid $\text{Bi}_{43}\text{Sn}_{57}$ sample (99.99% purity, Alfa Aesar) was prepared under UHV conditions ($P < 10^{-9}$ Torr). Atomically clean liquid surfaces were obtained by mechanical scraping and Ar^+ ion sputtering, as described previously [10, 14, 15]. Measurements were done using the liquid surface diffractometer at the ChemMatCARS beamline, Advanced Photon Source, Argonne National Laboratory at a sample temperature of $T = 142^\circ\text{C}$, 4°C above the $\text{Bi}_{43}\text{Sn}_{57}$ alloy's eutectic temperature, $T_e = 138^\circ\text{C}$.

The reflected intensity fraction, $R(q_z)$, of an x-ray beam impinging on a structured liquid surface at a grazing angle α , is given by the Born approximation as:

$$R(q_z) = R_F(q_z) \cdot |\Phi(q_z)|^2 \cdot CW(q_z) \quad (1)$$

where $q_z = (4\pi/\lambda)\sin\alpha$, λ is the x-ray wavelength, $R_F(q_z)$ is the Fresnel XR of an ideally abrupt and flat surface, $CW(q_z)$ is due to thermal surface capillary waves [9, 10], and the surface's structure factor is [16]:

$$\Phi(q_z) = \frac{1}{\rho_\infty} \int dz \frac{d\langle\rho(z)\rangle}{dz} \exp(iq_z z). \quad (2)$$

Here z is the surface-normal axis, ρ_∞ and $\rho(z)$ are the bulk and surface electron densities, respectively, and $\langle..\rangle$ denotes surface-parallel averaging. As R_F is a universal function depending only on the known critical angle for total external reflection, and $CW(q_z)$ is known accurately from capillary wave theory, the intrinsic density profile, $\langle\rho(z)\rangle$, is obtained by computer fitting the measured $R(q_z)$ by a physically motivated model described below [10].

The (forward) atomic scattering factor of a Z -electron atom varies with energy as [16]: $Z' = Z + f'(E) - if''(E)$, where $f'(E)$ and $f''(E) = \mu(E)\lambda/(4\pi)$, are the real and

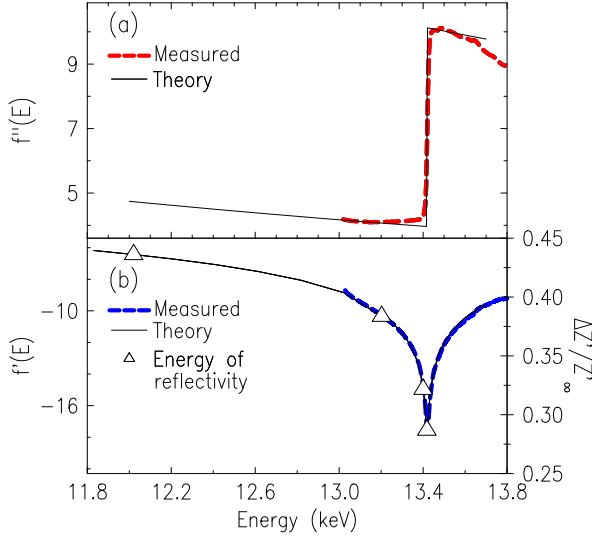


FIG. 1: Dispersion corrections (a) $f'(E)$ and (b) $f''(E)$ of Bi near the L3 absorption edge at $E_{L3} = 13.418$ keV. The right scale of (b) is the electron density contrast $\Delta Z'/Z'_\infty = (Z'_{Bi} - Z'_{Sn})/Z'_\infty$.

imaginary parts of the dispersion correction, and $\mu(E)$ is the photoelectric absorption coefficient.

The effect of f' on the analysis can be neglected and the changes in f' are significant only near an absorption edge. Fig. 1(a) shows $f''(E)$ near the Bi L3 edge as obtained from an absorption measurement in a Bi foil. Fig. 1(b) is the corresponding $f'(E)$, calculated from $f''(E)$ using the Kramers-Kronig relation [17]. Both agree well with theory [18, 19]. The composition dependence of $\langle \rho(z) \rangle$ was obtained by fitting the measured XR by the distorted crystal (DC) model for a layered liquid surface [7, 8]:

$$\frac{\langle \rho(z) \rangle}{\rho_\infty} = \sum_{n=1}^{\infty} \frac{e^{-(z-nd)^2/\sigma_n^2}}{\sqrt{2\pi}\sigma_n/d} \left(1 + \delta_n \frac{Z'_{Bi} - Z'_{Sn}}{Z'_\infty} \right) \frac{c_n}{c} \quad (3)$$

The progressive increase in the Gaussian width parameter $\sigma_n^2 = \sigma_0^2 + (n-1)\bar{\sigma}^2$ with increasing layer number n describes the layering amplitude's decay below the surface [8]. The layer spacing d is kept constant in this model due to similarity in size between Bi and Sn atoms. The bulk's average effective electron number per atom is $Z'_\infty = xZ'_{Bi} + (1-x)Z'_{Sn}$, and $\delta_n = x'_n - x$ is difference in the Bi fraction between the n -th layer, x'_n , and the bulk, x . The corresponding atomic densities, c_n and c , are determined from the atomic volumes v_{Bi} and v_{Sn} : $c_n x'_n v_{Bi} + c_n (1-x'_n) v_{Sn} = 1$. The contrast, $(Z'_{Bi} - Z'_{Sn})/Z'_\infty$, varies strongly near the edge due to the variation of Z'_{Bi} : from 0.43 at $E=12.00$ keV to 0.27 at $E=13.418$ keV (right axis in Fig. 1). This is the basis for the resonant XR method which allows to separate out the density profiles of the two species [4, 15].

Fig. 2 shows Fresnel-normalized XRs $R(q_z)/R_F(q_z)$

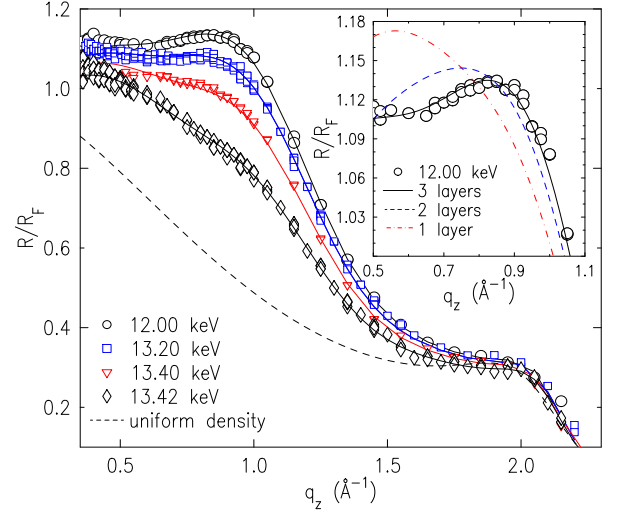


FIG. 2: XR measured at the indicated energies, with fits by the three-layer model (lines). The dashed line is the XR of a uniform-composition surface. Inset: The $E=12.00$ keV measured R/R_F with fits by the three models discussed in the text (lines). Error bars are smaller than the symbols' size.

measured near the Bi L3 edge at the four energies marked by triangles in Fig. 1(b). The dashed line is calculated from the DC model for a layered interface assuming a *uniform* composition ($\delta_n = 0$). The strong enhancement of the measured $R(q_z)/R_F(q_z)$ over this line, evidenced by the peak at $q_z \simeq 1.0 \text{ \AA}^{-1}$, and the strong energy-dependence of the low- q_z reflectivity, clearly indicate a significant surface segregation of Bi, and its variation with z .

Three fits of the data by the DC model, Eq. 3, were carried out, assuming that only one ($\delta_1 \neq 0, \delta_{n \geq 2} = 0$), two ($\delta_{1,2} \neq 0, \delta_{n \geq 3} = 0$), or three ($\delta_{1,2,3} \neq 0, \delta_{n \geq 4} = 0$) surface layers deviate from the bulk composition. All fits employed $d = 2.90 \text{ \AA}$, $\sigma_0 = 0.30 \text{ \AA}$ and $\bar{\sigma} = 0.57 \text{ \AA}$, derived from the energy-independent position, shape and intensity of the layering peak at $q_z = 2.0 \text{ \AA}^{-1}$. The measured $R(q_z)/R_F(q_z)$ of all four energies were fitted simultaneously, using the experimentally determined $f'(E)$.

Fig. 2 exhibits an excellent agreement of the three-layer model (solid lines) with the measurements, but a very poor agreement for the one- and two-layer models (inset). Table I lists the best-fit values of x'_n and $\delta_n^{Fit} = x'_n - x$ and the corresponding 95% non-linear confidence intervals $Y(x'_n)$ and $Y(\delta_n^{Fit})$ determined from a six-parameter support plane analysis [20]. The most striking result is the non-monotonic deviation δ_n of Bi from the 43% bulk value, showing an enhanced composition of 96% and 53% in the first and third layers, and depletion down to 25% in the second layer (see Fig. 3). Beyond the third layer entropy effects dominate the Gibbs adsorption and the layer and bulk concentrations can not be distinguished. While demixing has not been previously reported in liquid alloys, similar decaying oscillatory composition pro-

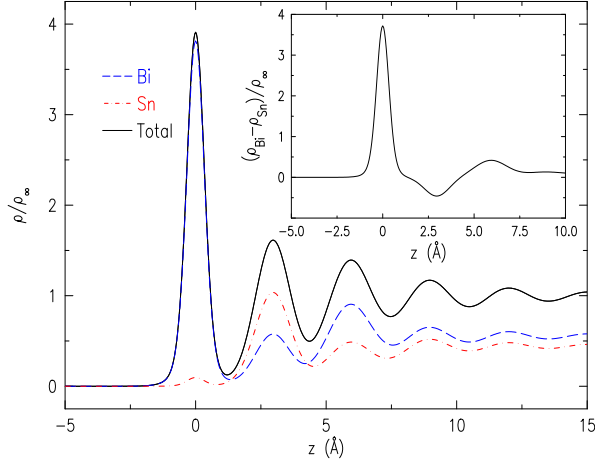


FIG. 3: Electron density profiles as derived from the fits to the reflectivities shown in Fig. 2. Inset: the bulk-normalized differences in electron density of Bi and Sn, $(\rho_{Bi} - \rho_{Sn})/\rho_\infty$.

files were discovered in several *crystalline* alloys such as Cu_3Au [21]. However, the properties, formation mechanism, and strong temperature dependence of the composition modulations in Cu_3Au alloys were found to be intimately related to, and largely dominated by, the long-range fcc order in the bulk crystal, and the severe packing strains resulting from the big mismatch in the atomic diameter of the two components. As none of these exist in our liquid alloy, surface-induced segregation and the Gibbs rule can be studied in a pure short-range-order interaction context, free from the complicating influence, or even dominance, of other effects. We now compare our experimental observations with theory.

Guggenheim's [22] application of Gibbs theory [1] to regular solutions assumes the surface segregation to be restricted to a single surface monolayer. Assuming p nearest neighbors for each bulk atom in a layered lattice model, lp are within, and mp are in the adjacent, layers. For a close-packed lattice, for example, $p = 12$, $l = 0.5$ and $m = 0.25$. The surface tension of the regular solution, γ_{AB} , follows from those of the pure components, γ_A and γ_B , as [22]:

$$\begin{aligned} \gamma_{AB} &= \gamma_B + \frac{kT}{a_B} \ln\left(\frac{1-x'}{1-x}\right) + \frac{\omega}{a_B} [lx'^2 - (l+m)x^2] \quad (4) \\ &= \gamma_A + \frac{kT}{a_A} \ln\left(\frac{x'}{x}\right) + \frac{\omega}{a_A} [l(1-x')^2 - (l+m)(1-x)^2]. \end{aligned}$$

Here, x and $(1-x)$ are the bulk concentrations of atoms A (Bi) and B (Sn), while $x' \neq x$ and $(1-x')$ are the corresponding surface concentrations, a_A and a_B are the two atomic areas, and $\omega = 2\omega_{AB} - \omega_{AA} - \omega_{BB}$ is the interaction parameter, defined by the A-B, A-A and B-B atomic interaction energies. Extrapolated down to $T = 142^\circ\text{C}$, $\gamma_{Bi} = 398$ mN/m and $\gamma_{Sn} = 567$ mN/m, while a_{Bi} and a_{Sn} are calculated from the atomic radii $r_{Bi} = 1.70$ Å and $r_{Sn} = 1.62$ Å assuming hexagonal close packing [23].

n	$x'_n(\text{Bi})$	$Y(x'_n)$	δ_n^{Fit}	$Y(\delta_n^{Fit})$	δ_n^{DP}	δ_n^{SK}
1	0.96	[0.94, 0.99]	0.53	[0.51, 0.56]	0.47	0.51
2	0.25	[0.18, 0.27]	-0.18	[-0.25, -0.16]	-0.23	-0.25
3	0.53	[0.50, 0.56]	0.10	[0.07, 0.13]	0.12	0.05
4	0.43	-	0	-	-0.06	-0.01

TABLE I: Density model parameters x'_n and $\delta_n^{Fit} = x'_n - x$, and confidence intervals $Y(x'_n)$ and $Y(\delta_n^{Fit})$ obtained from the three-layer model fits compared to theoretical δ_n^{DP} and δ_n^{SK} derived from the Defay-Prigogine and Strohl-King models.

Treating $\text{Bi}_{43}\text{Sn}_{57}$ as a perfect solution ($\omega/kT = 0$), the Gibbs theorem, Eq. 4, yields $\gamma_{AB} = 444$ mN/m and $x' = 0.904$, below the experimental value $x'_1(\text{Bi})$ in Table I. However, assuming a regular solution behavior with $\omega/kT = 1$ yields $\gamma_{AB} = 432$ mN/m, and $x' = 0.941$, which agrees very well with the experimentally derived $x'_1(\text{Bi})$ in Table I. Both γ_{AB} agree well with experiment and theory [24]. Note that γ_{AB} and x' are only weakly dependent on ω/kT due primarily to the logarithmic functional behavior and large surface tension difference of the two components, $a_{Sn}\gamma_{Sn} - a_{Bi}\gamma_{Bi} \approx 2 kT$. This introduces a large uncertainty of ω/kT calculated from measurements of surface tension or surface monolayer composition. Resonant XR measurements of sub-surface layer composition therefore present a unique opportunity to probe the nature of atomic interactions at the surface.

In spite of the good agreement above, confining the surface excess to a single monolayer is correct for perfect solutions only, but not for our case of a regular solution, as Defay and Prigogine [25] point out. They provide a correction for regular solutions, where the surface excess extends over two layers, the γ_{AB} values above do not change significantly and the layers' δ_n are related by:

$$\ln \frac{1 + \delta_2/x}{1 - \delta_2/(1-x)} - \frac{2\omega}{kT} \delta_2 - \frac{2\omega m}{kT} (\delta_1 - 2\delta_2) = 0. \quad (5)$$

Expanding Eq. 5 to first order in δ_2 :

$$\delta_2 = \frac{2\omega m x (1-x) \delta_1}{kT - 2\omega l x (1-x)}. \quad (6)$$

For nearly perfect solutions ($\omega/kT \ll 1$) Eq. 5 yields a negligible δ_2 : $0 < \delta_2 \ll \delta_1$. For $\omega/kT \gtrsim 1$, however, δ_2 and δ_1 are of opposite signs and $|\delta_2|$ may become comparable to $|\delta_1|$. This prediction is qualitatively consistent with the demixing observed here. For example, when $\omega/kT \gg 1$, Eq. 6 can be simplified further: $\delta_2 = -(m/l)\delta_1$. For $\text{Bi}_{43}\text{Sn}_{57}$, $m/l \approx 0.5$ and the Gibbs-predicted $x'_1 = 0.90$ (or $\delta_1 = 0.47$) yields $\delta_2 = -0.23$, $\delta_3 = 0.12$ and $\delta_4 = -0.06$ [26]. These values, shown as δ_n^{DP} in Table I, agree well with δ_n^{Fit} obtained from the three-layer model fits. The smallest value of the interaction parameter ω/kT for which satisfactory agreement with the Defay-Prigogine model could be obtained (by treating m as an adjustable parameter) is $\omega/kT = 2.3$.

Strohl and King [27] suggest a multilayer, multicomponent model, where no expansion is used, and x'_n are obtained iteratively, until convergence to a self-consistent composition profile is reached. A good agreement of this theory with our BiSn measurements is obtained when $\omega/kT = 1.0 - 1.7$. Typical δ_n^{SK} values are listed in Table I. As observed, the Strohl-King model provides composition profiles very similar to those of the Defay-Prigogine model, albeit with slightly different δ_n values, thus supporting our overall conclusions.

Theoretically, ω and the enthalpy of mixing, ΔH_m , are related by $\omega = \Delta H_m/[x(1-x)]$. In practice, however, bulk thermodynamic quantities were often found to yield inaccurate values for surface quantities. For example, organic [28] and metallic [29] mixtures exhibit significant disagreements between ω values derived empirically from surface tension measurements and from bulk calorimetry. For BiSn, reported values of ΔH_m range from endothermic values of 80 to 140 J/mol [12] to an exothermic value of -180 J/mol [13]. These values lead to $|\omega/kT| < 0.2$, i.e. an almost perfect solution, and an insignificant $|\delta_2| < 0.01$. On the other hand, the value of $\omega/kT \approx 10$ that we previously found necessary to account for the observed 35% Bi concentration enhancement at the surface monolayer at the BiIn eutectic is of the same order of magnitude as the value we find necessary to account for the present observation of surface segregation in BiSn, $\omega/kT \approx 1.0 - 2.3$. Unfortunately we do not have an explanation for the origin of the discrepancy in the values of ω/kT and this suggests an urgent need for both further theoretical studies of surface demixing as well as experimental investigations of similar effects in other binary alloys. In particular, the BiSn system appears to be the only liquid alloy for which clear evidence for multilayer surface demixing has been found. The case for new studies is strongly reinforced by the existence of a growing class of surface-induced ordering phenomena that have been observed in metallic liquids. In addition to the surface demixing reported here, these include layering [7, 8, 9, 10, 11], relaxation [11], segregation [2, 3, 4, 30], wetting transitions [14, 31], and surface freezing [32]. Finally, there is a basic unresolved question of whether the surfaces of liquid metals are fundamentally different from those of non-metallic liquids [33].

This work has been supported by the U.S. DOE grants No. DE-FG02-88-ER45379, DE-AC02-98CH10886 and the U.S.-Israel Binational Science Foundation, Jerusalem. We gratefully acknowledge useful discussions with E. Sloutskin at Bar-Ilan as well as assistance from T. Graber, D. Schultz and J. Gebhardt at ChemMatCARS Sector 15, principally supported by the NSF/DOE grant No. CHE0087817. The Advanced Photon Source is supported by the U.S. DOE contract No. W-31-109-Eng-38.

Laboratory, Argonne, IL, 60439

- [1] J. W. Gibbs *et al.*, *The collected works of J. Willard Gibbs* (Longmans, New York, 1928).
- [2] M. J. Regan *et al.*, Phys. Rev. B **55**, 15874 (1997).
- [3] E. DiMasi *et al.*, MRS Symp. Ser. **590**, 183 (2000).
- [4] E. DiMasi *et al.*, Phys. Rev. Lett. **86**, 1538 (2001).
- [5] K. N. Tu *et al.*, J. Appl. Phys. **93**, 1335 (2003); J. Glazer, Int. Mat. Rev. **40**, 65 (1995).
- [6] J. G. Lee and H. Mori, Phys. Rev. B **70**, 144105 (2004).
- [7] O. M. Magnussen *et al.*, Phys. Rev. Lett. **74**, 4444 (1995).
- [8] M. J. Regan *et al.*, Phys. Rev. Lett. **75**, 2498 (1995).
- [9] H. Tostmann *et al.*, Phys. Rev. B **59**, 783 (1999).
- [10] O. G. Shpyrko *et al.*, Phys. Rev. B **67**, 115405 (2003).
- [11] O. G. Shpyrko *et al.*, Phys. Rev. B **70**, 224206 (2004).
- [12] N. A. Asryan and A. Mikula, Inorg. Mat. **40**, 386 (2004); R. Hultgren *et al.*, *Selected Values of the Thermodynamic Properties of Binary Alloys* (Metals Park, OH, 1973); R. L. Sharkey and M. J. Pool, Metall. Trans. **3**, 1773 (1972); H. Seltz *et al.*, J. Am. Chem. Soc. **64**, 1392 (1942).
- [13] S. A. Cho and J. L. Ochoa, Metall. Mater. Trans. B **28**, 1081 (1997).
- [14] P. Huber *et al.*, Phys. Rev. Lett. **89**, 035502 (2002).
- [15] O. G. Shpyrko, Ph.D. thesis, Harvard University, 2003 (unpublished).
- [16] J. Als-Nielsen and D. McMorrow, *Elements of Modern X-ray Physics* (Wiley, New York, 2001).
- [17] G. Evans and R. F. Pettifer, J. Appl. Cryst. **34**, 82 (2001); J. J. Hoyt *et al.*, J. Appl. Cryst. **17**, 344 (1984).
- [18] E. A. Merritt, Anomalous Scattering Coefficients, <http://www.bmsc.washington.edu/scatter/> (1996-2003).
- [19] M. Newville, computer code IFEFFIT, (1997-2004).
- [20] P. R. Bevington and D. K. Robinson, *Data Reduction and Error Analysis for the Physical Sciences* (McGraw-Hill, New York, 1992) p. 212.
- [21] H. Reichert *et al.*, Phys. Rev. Lett. **78**, 3475 (1997); *ibid* **74**, 2006 (1995); *ibid* **90**, 185504 (2003).
- [22] E. A. Guggenheim, Trans. Faraday Soc. **41**, 150 (1945).
- [23] *CRC Handbook of Chemistry and Physics*, ed. by D. R. Lide (CRC, Boca Raton, 1996).
- [24] S. W. Yoon *et al.*, Script. Mat. **40**, 297 (1999).
- [25] R. Defay and I. Prigogine, Trans. Far. Soc. **46**, 199 (1950).
- [26] Eq. 6 yields δ_3 from δ_2 and δ_4 from δ_3 .
- [27] J. K. Strohl and T. S. King, J. Catal. **118**, 53 (1989).
- [28] G. L. Gaines, Trans. Far. Soc. **65**, 2320 (1969).
- [29] T. P. Hoar and D. A. Melford, Trans. Far. Soc. **53**, 315 (1957).
- [30] E. B. Flom *et al.*, Science **260**, 332 (1993).
- [31] H. Shim *et al.*, Surf. Sci. **476**, L273 (2001); A. H. Ayyad and W. Freyland, *ibid.* **506**, 1 (2002).
- [32] A. Issanin *et al.*, J. Chem. Phys. **121**, 12005 (2004); B. Yang *et al.*, Phys. Rev. B **62**, 13111 (2000); O. G. Shpyrko *et al.*, in preparation (2005).
- [33] E. Chacón and P. Tarazona, Phys. Rev. Lett. **91**, 166103 (2003); D. X. Li and S. A. Rice, J. Phys. Chem. B **108**, 19640 (2004); O. G. Shpyrko *et al.*, Phys. Rev. B **69**, 245423 (2004).

* Electronic address: oleg@xray.harvard.edu; present address: Center for Nanoscale Materials, Argonne National